Journal of the Nigerian Mathematical Society
Vol. 41, Issue 3, pp. 287-312, 2022

IMPACT OF ENTROPY GENERATION ON HYDROMAGNETIC NANOFLUID FLOW DISPERSED OVER A RADIATIVE VERTICAL POROUS PLATE WITH NEWTONIAN HEATING

A. J. OMOWAYE AND O. K. KORIKO

ABSTRACT. Recently and over the years, the industrial applications of second law analysis is becoming famous. Hence, this work intend to address the combined impacts of water-based nanofluids, convective boundary state, thermal radiation, magnetic field and second law of thermodynamics. The governing equations that unravel the flow within the boundary layer are provided. The transformed governing equations are obtained by guided similarity variables, the transformed equations are solved analytically by method of undetermined coefficient. Entropy generation rate and Bejan number in dimensionless form are obtained by deriving an expression through the analytical solutions of temperature and velocity. The emerging parameters of the flow are: Bejan number, Biot number, radiation parameter, entropy generation rate, skin friction, Hartman number, suction, Prandtl, Nusselt and Reynolds number. Also, the effects of these parameters are presented in graphs and tables. In addition, Entropy generation are enhanced by Eckert number, radiation parameter, permeability parameter, suction , prandtl number and Brinkman number for both copper and alumina water. Finally, the results of this work is compared with published work in the literature, this result is in consonant with this work.

Keyword:Entropy generation, MHD, nanofluid, radiation, Newtonian heating. 2010 Mathematical Subject Classification: 76D10; 76S05; 76W05

Received by the editors May 11, 2021; Revised: October 17, 2022; Accepted: October 25, 2022

www.nigerianmathematicalsociety.org; Journal available online at https://ojs.ictp.it/jnms/

1. INTRODUCTION

The word nanofluid was coined and used by Choi (1995) to mean dispersion of metallic or non - metallic nanoparticles of size less than one hundred nanometer in base fluid that could be oil, water, etc. This class of fluid gives an efficient lubricant, coolants for many industry. Recently, nanoparticles has been an area of research interest to many researchers due to its usefulness in biomedical and applied sciences. It is interesting to note that when nanoparticles are dissolved in a base fluid the mixture enhanced heat transfer in a fluid. Khan and Pop (2010) reported the flow of nanofluid on stretched sheet. Eshetu and Shankar (2014) carried out a numerical study of heat, mass flows of viscous nanofluid on vertical stretched sheet in a magnetic, thermal radiating environment; the nanoparticles volume fraction reduced as a result of Lewis number. Keblinski *et al.* (2002) investigated the process of heat movement in a fluid containing particles which has a Nano-Sized in diameter. Buongiorno(2006) conducted a study on the characteristics of heat transferred effects on nanoparticles mass transfer in a nanofluid. Sheikholeslami *et al.* (2015) proposed two phase model to study the effects of radiation on nanofluid. Nanofluid pumping and thermal power was carried out by Akbarzadeh *et al.* (2016) using the sensitivity analysis. Zainal *et al.* (2020) investigated MHD hybrid nanofluid flow with radiation in a moving permeable porous surface. Finding showed that magnetic field and suction slow down the movement of the fluid due to relationship between the electric and magnetic field which brings about Lorentz force. While radiation escalation enhanced the heat movement rate in the medium. More so, dual solutions exist and the stability analysis on the solution revealed that only one of the solutions was physically useful.

The research on the influence of magnetic field is of great importance in engineering at the same time in science. Ever since the advent of Alfven (1942) who reported the usefulness of MHD in many areas of study and field such as aerodynamics, Geophysics, bearing, microelectronic devices, etc. The presence of MHD in the Navier-Stokes equation of motion is only correct when we assumed the magnetic Reynold number too small, hence induced magnetic field is neglected. Omowaye (2016) provided an existence results for a system of differential equations describing the flow of a reacting fluid in a porous plate under the influence of magnetic field. Omowaye (2011) explored a steady MHD reacting convective fluid flow in a bounded domain. The existence and unique of solutions were provided for the problem. Results showed that velocity increased as a result of as Grashof number, Frank-Kamenetskii, and Prandtl number.

Furthermore, for the design of any thermal systems to work optimally, it is important to note that nanofluids can be used to enhance the heat transfer rate at the same time the entropy generation need to be minimised (Bejan, 1996). It is a known fact that during entropy generation, the amount of energy in the system and thermal system decreases thereby diminishes the rate of efficiency. When we considered the first and second laws of thermodynamics, the first explained the principle of conservation of energy while the second talks about irreversibility of all real process. The irreversibility of a thermodynamics system can be measure by its entropy generation rate vis and vis the energy increases while exergy decreases. The entropy production in a system is enhanced by mass transfer, viscous dissipation, etc by virtue of interaction at the solid surfaces (Woods, 1975). Also, the volume of energy in a system is a function of entropy generation within the system. Hence, when entropy generation is minimised, then heat systems is optimised to get maximum heat transfer and there is drop in pressure to the minima level. In an engineering process that can not be reversed the entropy generated depreciates by virtue of irreversibilities of the process. More so, the entropy generation is a measure of quantitative irreversibilities as a result of thermodynamic process. This is used as a condition for effective performance of engineering equipments. In other words, it is looked at as a random movement of molecules propagated in a fluid flow, mass and heat transfer [Kish and Ferry(2017), Narayan *et al.* (2010), Datta *et al.* (2016)]. Information on entropy generation in various thermal system see [Bejan, 1995, Bejan, 1982]. Monaledi and Makinde (2019) investigated the thermal performance of water-copper nanoparticle shape with volume fraction and inherent irreversibility. The results showed that volume fraction and nanoparticles shapes affected the entropy generation. Zainal *et al.* (2020) investigated MHD hybrid nanofluid flow with radiation in a moving permeable porous surface. Finding showed that magnetic field and suction slow down the movement of the fluid due to relationship between the electric and magnetic field which brings about Lorentz force. While radiation escalation enhanced the heat movement rate in the medium. More so, dual solutions exist and the stability analysis on the solution revealed that only one of the solutions was physically useful.

Sahoo and Nandkeolyar (2021) elucidated on entropy generated by MHD Casson mixed convection flow of nanofluid and hall current in contact with thermal radiation. Analysis showed that the Casson parameter behaved as helping parameter in the temperature field when viscous and Joule dissipation are not there. Also, for large Brinkman number entropy generation increases rapidly. Finally, in other to improve the effectiveness of the model a multiple regression analysis was carried out for those physical quantities present in the model.

Newtonian heating refers to movement of heat from the surface of a plate, this heat is proportional to surface temperature. However, over the years owing to the usefulness and industrial applications of Newtonian heating scientists, engineers has included the condition in their respective studies. Oluwakuade, *et al.* (2019) took Newtonian heating into consideration and explored a steady reacting MHD convective fluid flow on a vertical surface. The velocity and temperature of the fluid increased as a result of Biot number. The effect of Newtonian heating on a boundary layer natural convective viscous fluid flow on a vertical surface was considered by Merkin (1994).Hussanan *et al.* (2013) reported Newtonian heating influence on heat and mass transfer on a vertical plate, the exact solution of the problem was obtained and the results of the flowing parameters were provided graphically. Hussanan *et al.* (2014) employed Laplace transform method to solve boundary layer flow with Newtonian heating of a Casson fluid in contact with thermal radiation. Vieru *et al.* (2014) provided an analytical results of MHD Newtonian heating on mass diffusion in a stress shear viscous convective fluid flow on an infinite plate. While Ramzan (2015) presented the influence of Newtonian heating on couple stress nanofluid flow of MHD in 3-D in the presence of Joule heating and viscous dissipation.

Therefore, fascinated and inspired by the applications of these studies above, the present study will explore the impact of entropy generation on hydromagnetic nanofluid flow dispersed over a radiative vertical porous plate with Newtonian heating. Of particular interest in this study is the analytical solution of the the problem which serves as a check on asymptotic and numerical solution. The present study will be compared with that of Ajala *et al.*(2019) in a particular case. The physical characteristics of the flow parameters are annotated in graphs for better understanding.

2. FORMULATION

Suppose we consider a steady flow of an electrically conducting nanofluid flow dispense over a radiative infinite vertical porous plate with Newtonian heating. Initially the plate is moving with a velocity of U_0 in its own plane while the axis -y is taken along the flow as shown in figure 1. The nanoparticles and the base fluid (water) are in thermal equilibrium and there is no slip condition. A magnetic field B_0 of uniform strength is applied normal to the flow while the viscous dissipation is taken into consideration assume magnetic Reynolds number to be small. Following the nanofluid model of Ajala *et al.* (2019) and invoking the Boussinesq approximation. Then the governing equation is given as:

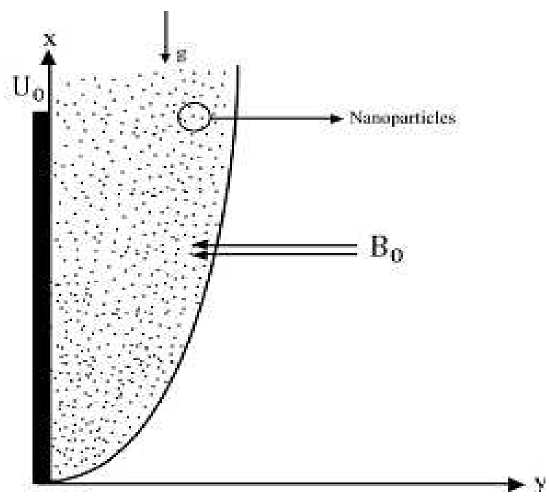

Figure 1: Geometry of the flow.

$$\frac{\partial v}{\partial y_1} = 0 \tag{2.1}$$

$$v\frac{\partial u_1}{\partial y_1} = \frac{\mu_{nf}}{\rho_{1nf}}\frac{\partial^2 u_1}{\partial y_1^2} - \frac{\sigma_{1nf}}{\rho_{1nf}}\beta_0^2 u_1 - \frac{\nu_{1nf}}{k}u_1 \tag{2.2}$$

$$v\frac{\partial T_1}{\partial y_1} = \frac{k_{1nf}}{(\rho_1 c_p)_{nf}}\frac{\partial^2 T_1}{\partial y_1^2} + \frac{\mu_{1nf}}{(\rho c_p)_{1nf}}\left(\frac{\partial u_1}{\partial y_1}\right)^2 + \frac{\sigma_{nf}}{(\rho c_p)_{1nf}}\beta_0^2 u_1^2 - \frac{1}{(\rho c_p)_{1nf}}\frac{\partial q_r}{\partial y_1} \tag{2.3}$$

with the boundary conditions

$$\begin{array}{llll} u_1(y_1) = u_0 & -k_{1nf}\frac{dT_1}{dy_1} = h_f(T_f - T_1) & at & y_1 = 0 \\ u_1(y_1) \to u_\infty & T_1(y_1) \to T_\infty & & y_1 \to \infty \end{array} \tag{2.4}$$

where u_1 is the velocity of the fluid, T_1 nanofluid temperature, v0 suction velocity, T_∞ is the temperature at free stream, α_{1nf}thermal diffusivity of nanofluid that is given as

$$\alpha_{1nf} = \frac{k_{1nf}}{(\rho c_p)_{1nf}} \tag{2.5}$$

μ_{1nf} is the dynamic viscosity of the nanofluid, the nanofluid density ρ_{1nf} given in Brinkman(1952)

$$\rho_{1nf} = (1-\xi)\rho_f + \xi\rho_s \qquad \mu_{1nf} = \frac{\mu_f}{(1-\xi)^{2.5}} \qquad \sigma_{1nf} = \sigma_f\left(1 + \frac{3((\frac{\sigma_s}{\sigma_f}) - 1)\xi}{(\frac{\sigma_s}{\sigma_f} + 2) - (\frac{\sigma_s}{\sigma_f})\xi}\right) \tag{2.6}$$

the nano-particle volume fraction is ξ,ρ_f, ρ_s base fluid and solid particle densities, σ_f, σ_s the base fluid and nano-particle of electrical conductivity respectively and $\mu_f$viscosity of base fluid. While the thermophysical properties of the base fluid and nanoparticles are given in table 1.

Table 1: Thermophysical properties of base fluid and nanoparticles (Oztop and Abu-Nada,2008)

Physical properties	H_2O	Al_2O_3	Cu
$\rho(k/m^3)$	997.1	3970	8933
$C_p(J/kgK)$	4179	756	385
K(W/mK)	0.613	40	400
$\beta(K^{-1})$	21X10^{-5}	0.85X10^{-5}	1.67X10^{-5}

Aminossa and Ghasemi(2019) define the nanofluid thermal conductivity as

$$\frac{k_{1nf}}{k_f} = \frac{(k_s + 2k_f) - 2\xi(k_f - k_s)}{(k_s + 2k_f) - \xi(k_f - k_s)} \tag{2.7}$$

(ρc_p) nanofluid capacitance is given by

$$(\rho c_p) = (1-\xi)(\rho c_p)_f + \xi(\rho c_p)_s \tag{2.8}$$

the subscripts in equ (2.5)- equ(2.8) are basic features of the base fluid, nanofluid nano-particle.

The Roseland approximation is used to illustrate the radiative heat flux, this is given in Fagbade *et al.* (2018) as

$$\frac{dq_r}{dy_1} = \frac{-4\sigma_1}{k_1^*}\frac{dT_1^4}{dy_1} \approx \frac{-16\sigma_1 T_\infty^3}{3k_1^*}\frac{d^2T_1}{dy_1^2} \tag{2.9}$$

Introducing non-dimensional variables

$$\varsigma = \frac{y_1 u_0}{\nu_f} \qquad \Theta = \frac{T_1 - T_\infty}{T_f - T_\infty} \qquad M = \frac{u_1}{u_0} \tag{2.10}$$

Substituting equations (2.5)-(2.10) into equations (1)-(3) we have

$$\frac{d^2M}{d\varsigma^2} - S\Gamma_1 \frac{dM}{d\varsigma} - \Gamma_2 M - k_1 M = 0 \tag{2.11}$$

$$\Gamma_3 \frac{d^2\Theta}{d\varsigma^2} - S\Gamma_4 \frac{d\Theta}{d\varsigma} + \Gamma_5 \left(\frac{dM}{d\varsigma}\right)^2 + \Gamma_6 M^2 = 0 \tag{2.12}$$

where $\Gamma_1 = \frac{(1-\xi)^{2.5}((1-\xi)\rho_f + \rho_s \xi)}{\mu_f}$, $\Gamma_2 = (1-\xi)^{2.5}\left(1 + \frac{(3\frac{\sigma_s}{\sigma_f}-1)\xi}{(\frac{\sigma_s}{\sigma_f}+2)+((\frac{\sigma_s}{\sigma_f})-1)}\right) H_a^2$,
$k_1 = \frac{\nu_f^2}{ku_0^2}$

$\Gamma_3 = (1 + \frac{4}{3}N\left(\frac{(k_s+2k_f)-2\xi(k_f-k_s)}{(k_s+2k_f)-\xi(k_f-k_s)}\right))(\frac{(\rho c_p)_f \frac{(k_s+2k_f)-2\xi(k_f-k_s)}{(k_s+2k_f)-\xi(k_f-k_s)}}{pr(1-\xi+\frac{\xi(\rho c_p)_f}{(\rho c_p)_s})})$

$\Gamma_4 = \frac{\rho_f Ec}{(1-\xi)\rho_f + \xi\rho_s(1-\xi)^2.5}$, $\Gamma_5 = \left(1 + \frac{3((\rho_s/\rho_f)-1)\xi}{((\rho_s/\rho_f)+2)-((\rho_s/\rho_f)-1)\xi}\right)(1-\xi)^{2.5} Ha^2 Ec$. where S the suction parameter, Pr Prandtl number, Ha Hartman number, k_1 porosity parameter, N radiation parameter, Ec Eckert number.

The boundary conditions are

$$M(\varsigma) = 1 \qquad \frac{k_{nf}}{k_f}\Theta'(\varsigma) = Bn(\Theta(\varsigma)-1) \qquad \varsigma = 0 \tag{2.13}$$

$$M(\varsigma) \to 0 \qquad \Theta(\varsigma) \to 0 \qquad \varsigma \to \infty \tag{2.14}$$

where $Bn = \frac{\nu_f h_f}{k_f}$ is the Biot number.

3. METHOD OF SOLUTION

Equations (2.11) and (2.12) subject to equations (2.13) and (2.14) are solved analytically using method of undetermined coefficient. The results are presented as

$$M(\varsigma) = e^{-a_1\varsigma} \tag{3.1}$$

$$\Theta(\varsigma) = a_2 e^{-a_3\varsigma} + a_4 e^{-2a_1\varsigma} \tag{3.2}$$

where $a_1, ..., a_5$ are defined in the appendix.

The skin friction coefficient S_f and Nusselt number Nn_x are parameters of interest to engineers they are given as:

$$S_f = \frac{\tau_w}{\rho_f u_w^2} \quad , \quad Nn_x = \frac{xq_w}{k_f(T_w - T_\infty)} \tag{3.3}$$

where

$$\tau_w = \mu_{nf}\left(\frac{\partial u_1}{\partial y_1}\right)_{y_1=0} q_w = -k_{nf}\left(\frac{\partial T_1}{\partial y_1}\right)_{y_1=0} \tag{3.4}$$

using (2.10) in (3.3) and (17) yields

$$S_f Rex^{1/2} = \frac{1}{(1-\xi)^{2.5}} M'(0) \qquad Nnx \Big/ Rex^{1/2} = -\frac{k_{nf}}{k_f}\Theta'(0) \tag{3.5}$$

4. ENTROPY GENERATION

Following (Bejan(1996), Alboud and Saouli(2010), Monaledi and Makinde(2019)), the rate of generation of entropy of a nanofluid, when magnetic field, thermal radiation is presented over an infinite vertical plate using the boundary layer approximations is given by

$$S_{gen} = \frac{k_{nf}}{T_\infty^2}\left(1+\frac{16\sigma_1 T_\infty^3}{k^* k_f}\frac{k_{nf}}{k_f}\right)\left(\frac{dT_1}{dy_1}\right)^2 + \frac{\mu_{nf}}{T_\infty}\left(\frac{du_1}{dy_1}\right)^2 + \frac{\sigma_{nf}\beta_0^2 u_1^2}{T_\infty} \tag{4.1}$$

The entropy generation rate due to characteristic length is given by

$$S_0 = \frac{k(\Delta T_1)^2}{L^2 T_\infty^2} \tag{4.2}$$

Entropy generation in a dimensionless form can be expressed as

$$Q = \frac{S_{gen}}{S_0} = Re_L \Gamma_3 \left(\frac{d\Theta}{d\varsigma}\right)^2 + \Gamma_6 Re_L \frac{Br}{\Omega}\left(\frac{dM}{d\varsigma}\right)^2 + \Gamma_7 Re_L Ha \frac{Br}{\Omega} M^2 \tag{4.3}$$

where $Re_L = \frac{L^2 u_0^2}{\nu_f^2}$ Reynolds number, $Br = \frac{\mu_f u_0^2}{k_f \Delta T}$ Brinkman number, $\Omega = \frac{\Delta T}{T_\infty}$ dimensionless temperature parameter, $\Delta T = (T_f - T_\infty)$ temperature difference, $\Gamma_6 = \frac{k_s+2k_f-\xi(k_f-k_s)}{k_s+2k_f-2\xi(k_f-k_s)(1-\xi)^{2.5}}$,
$\Gamma_7 = \left(1+\frac{3((\frac{\sigma_s}{\sigma_f})-1)\xi}{(\frac{\sigma_s}{\sigma_f}+2)-(\frac{\sigma_s}{\sigma_f}-1)\xi}\right)$
we can rewrite equ (4.3) as

$$Q = P_1 + P_2 \tag{4.4}$$

where $P_1 = Re_L \Gamma_3 \left(\frac{d\Theta}{d\varsigma}\right)^2$ and $p_2 = \Gamma_6 Re_L \frac{Br}{\Omega}\left(\frac{dM}{d\varsigma}\right)^2 + \Gamma_7 Re_L Ha \frac{Br}{\Omega} M^2$ This implies P1 is heat transfer due to irreversibility while p2 is entropy generation by the friction due to the fluid and the magnetic field. Then the Bejan number is given as

$$Be = \frac{p_1}{Q} = \frac{1}{1+\varphi} \tag{4.5}$$

where $\varphi = \frac{p_2}{p_1}$ is the irreversibilty ratio. We must remark here that the irreversibility is major when $\varphi > 1$ while irreversibility due to heat transfer is dominant for $0 < \varphi < 1$. Finally, $\varphi = 1$when irreverssibity due to heat transfer and friction are the same. It is obvious from the above equation that Bejan number is between 0 and 1. The Bejan number will be the same as at the boundary when Be=0 this implies irreversibilty is by heat transfer. Be=1 depicts boundary at which irreversibility is dominated by friction in the flow. It is equivalent at Be=0.5 when friction and heat transfer are the same.

Table 2. Values of -$M^{'}(0)$ for different values of S are compared with results obtained by Ajala *et al.*(2019).

S	- $M^{'}(0)$ $k_1 = Ha$=Bn=Re=Ω=0.1,Ec=0.01,Nr=1.0,Br=0.8,Pr=0.71	
	Ajala *et al* (2019)	Present work
0.1	1.7563	1.75633660
0.3	1.8622	1.86218711
0.5	1.9738	1.97382853

Table 3. Values of skin friction coefficient and nusselt number at various values of Hartman number

Bn	$\frac{1}{(1-\xi)^{2.5}}M^{'}(0)$	- $-\frac{k_{nf}}{k_f}\Theta^{'}(0)$
0.1	-1.756336596381	0.031403584884
0.3	-2.644176875511	0.238731853004
0.5	-3.2977565696451991	0.718920340300

5. ANALYSIS AND DISCUSSION OF RESULTS

The problem of impact of entropy generation on hydromagnetic nanofluid flow dispersed over a radiative vertical porous plate with Newtonian heating is explored in this work. Equations (2.11) and (2.12) together with equations (2.13) and (2.14) are solved analytically by an efficient method called undermined coefficient. The solutions of equations (3.1) and (3.2) are discussed and annotated in graphs to infer the behaviour of emerging parameters in the flow regime. The analytical solutions (3.1) and (3.2) are substituted into (4.3) where expression for entropy generation rate along the vertical plate is obtained. Visible among the parameters are prandtl number, permeability parameter, magnetic parameter, Eckert number, Bejan number, suction, radiation parameter, Reynolds number, Brinkman number among others. Furthermore, values of these parameters are carefully selected in conjunction with standard values of these parameters in the literature. Also, in both cases of velocity and temperature profiles the dash line indicates the copper water while the solid line indicate the alumina water.

Also, to validate the present study in limiting cases, this work was compared with Ajala *et al*(2019), the results we obtained in table 2 encourage us, in that this result is in agreement with that of the published work Figures 2-8 elucidate the significance of the flow parameters on the temperature and velocity variation during the flow. The variation of permeability parameter on the velocity and temperature profiles for both cases of copper and aluminia water are depicted in figures 2 and 3. The velocity decreases as permeability parameter increases for both copper and alumina water. This indicates that more of the fluid are drainig away quickly from the pores of the plate while the temperature of the fluid decreases as permeability parameter increases, it is also observe that alumina water retain more heat than the copper water. Figures 4 and 5 indicate the variation in velocity and temperature plots for different values of Suction/injection parameter. It is observed that increase in Suction/injection parameter leads to drastic reduction in the momentum and thermal boundary layer for both $Al_2O_3 - water$ and $Cu-water$ nanofluids. Figure 6 exhibits the influence of Biot number (Bn) on temperature distribution. The Biot number is defined as the rate of change in temperature which is directly proportional to the difference in temperature of the fluid and temperature of the nanofluid. It is discovered that the Biot number is an increasing function of the thermal boundary layer for both $Al_2O_3-water$ and $Cu - water$ nanofluids. The reason can be attributed to the fact that the values of the Biot number in consideration are relatively small (Bn < 1) and are thermally simple, due to uniform temperature distributions that is applied to its body surface. The effect of Eckert number (Ec) on temperature field is portrays in figure 7. The Eckert number is the ratio of flow's kinetic energy to the enthalpy. It is found that temperature of the flow decreases, this is because of internal friction within the boundary layer which try to retards the flow of heat in the system as in the case of $Al_2O_3-water$ as well as $Cu-water$. Figure 8 illustrates the impact of Radiation parameter (Nr) on the thermal field. It is obvious that increase in Radiation parameter enhances the thermal boundary layer for both $Al_2O_3 - water$ and $Cu - water$ nanofluids. Prandtl number (Pr) influence on the temperature field is displayed in figure 9. It is obvious that an increase in the Prandtl number propels the thermal boundary layer for both $Al_2O_3 - water$ and $Cu - water$ nanofluids. This is due to the fact that higher Prandtl number implies enhancement in the thermal conductivity and the efficiency of heat transfer system of the fluid.

The influence of some parameters on Bejan number are displayed in figures 9-17. Figure 9 illustrates the effect of Suction/injection parameter (S) on Bejan number (Be). It is observed that the Suction/injection parameter is an increasing function of the Bejan number due to heat transfer irreversibility dominance at the Suction wall. The variation of permeability parameter (K_1) on Bejan number (Be) is displayed in figure 10. It is found that the rise in permeability parameter leads to value increase in Bejan number. The reason can be attributed to heat transfer irreversibility dominance over fluid friction irreversibility within the porous medium. Also, this effect is more noticeable in the alumina water than copper water. Figure 11 depicts the impact of Biot number (Bn) on Bejan number (Be). It is observed that biot parameter enhanced the Bejan number. Physically, Biot number connotes the relative importance of conduction and convection which determines the temperature difference during convection and by conductive transport rate it encourages heat transfer by irreversibility. Also, the alumina water Bejan number is higher than that of copper water. The impact of Eckert number (Ec) on Bejan number is shown in Figure 12. It is noticed that increase in Eckert number gives rise to increase in Bejan number, which indicates the relationship between enthalpy and flow kinetic energy of the fluid. Figure 13 expressed the influence of thermal radiation parameter (Nr) on Bejan number (Be). It is observed that the Bejan number is an increasing function of thermal radiation parameter, this is due to heat transfer irreversibility dominance over entropy generation. Figure 14 displays the influence of Prandtl number (Pr) on Bejan number (Be). It is observed that Prandtl number is an increasing function of the Bejan number. This is as a result of heat transfer irreversibility dominance over fluid friction irreversibility. Figure 15 shows the effect of Brinkman number (Br) on Bejan number (Be). It is found that the Brinkman number is a decreasing function of the Bejan number which indicates reduction in heat transfer as a result of fluid friction irreversibility dominance over heat transfer irreversibility. Figure 16 displays the effect of dimensionless temperature parameter (Ω) on Bejan number (Be). The dimensionless temperature parameter (Ω) is an increasing function of Bejan number due to extra source of heat coming to the system. Also, it encourages heat transfer by irreversibility. Figure 17 shows the effect of Hartman number (Ha) on Bejan number (Be). It is noticed that increase in Hartman number implies a rise in Bejan number for copper water while it has little or no effect on alumina water.

The outcome of some pertinent parameter on the entropy generation rate are portray in figures 18-23. Figure 18 displays the effect of Suction/injection parameter (S) on entropy generation rate (Q). It is noticed that increase in the Suction/injection parameter gives rise to generation rate. This is as a result of Suction on the fluid system encourages entropy generation. Figure 19 shows the influence of permeability parameter (K_1) on entropy generation rate (Q). It is discovered that the permeability parameter is an increasing function of the entropy generation rate. Also, the entropy generation rate is higher in copper water between $0 \leq Q \leq 0.5$ while that of alumina water is higher between $0.5 \leq Q \leq 1$. Figure 20 illustrates the effect of Eckert number on entropy generation rate (Q). It is noticed that there is an overlapping both in the profiles of copper and alumina water between $0 \leq Q \leq 0.5$, also the entropy generation is higher in copper water at the initial stage than alumina water. Between $0.5 \leq Q \leq 1$ the entropy generation rate for alumina water is higher than that of copper water. Figure 21 depicts the impact of thermal radiation parameter on entropy generation rate (Q). It is found that increase in thermal radiation parameter is to increase entropy generation rate this can be attributed to increase in radiation emission. It is observed that the profiles of copper and alumina water supper imposes between $0.3 \leq Q \leq 0.5$ beyond this region that is $Q = 0.5$ the entropy generation rate for alumina water is higher than that of copper water. The effect of Prandtl number (Pr) on entropy generation rate (Q) is displayed in figure 22. It is noticed that an increase in Prandtl number makes the entropy generation rate to increase due to entropy generation dominance over fluid friction irreversibility. The figure also portray that entropy generation rate is well pronounced in alumina water in terms of the Prandtl number than any other parameter. Figure 23 illustrates the influence of Brinkman number on entropy generation rate (Q). It is noticed that increase in Brinkman number value increases entropy generation rate. Furthermore, the entropy generation rate is higher in copper water than alumina water more so, their entropy rate is very close between $0 \leq Q \leq 0.3$ and try to converge at the free stream. Table 3 shows the effect of Hartman number on the skin friction and Nusselt number as Hartman number increases the Nusselt number increases while the skin friction decreases. Table 4 portrays the Bejan and entropy generation rate together with various fluid conditions and fluid properties. It is obvious that both Bejan and entropy rate decreases for both alumina and copper water when suction, permeability parameter, Eckert number increases while the reverse is the case for biot number, radiation parameter and Prandtl number.ix

6. APPENDIX

$a_1 = \frac{S\gamma_1+\sqrt{((S\gamma_1)^2+4(\gamma_2+k_1))}}{2}$,$a_2 = -(a_3 + a_5)$,$a_4 = -\frac{S}{\gamma_3}$,$a_5 = -\frac{(a_1^2\gamma_4+\gamma_5)}{4\gamma_3 a_1^2+2a_1 S}$, $a_3 = \frac{(\frac{k_f}{k_{nf}}Bi(\theta(0)-1))+2a_1 a_5}{-a_4}$

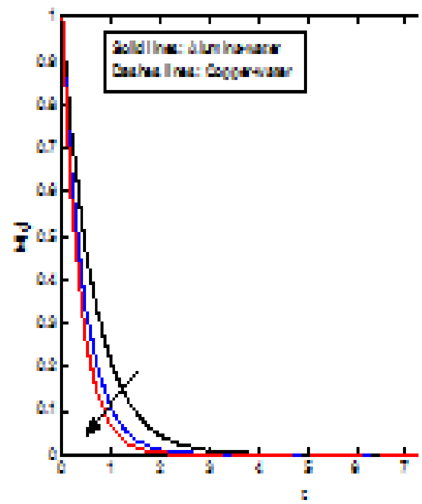

Figure 2: Variation of velocity profiles with k_1

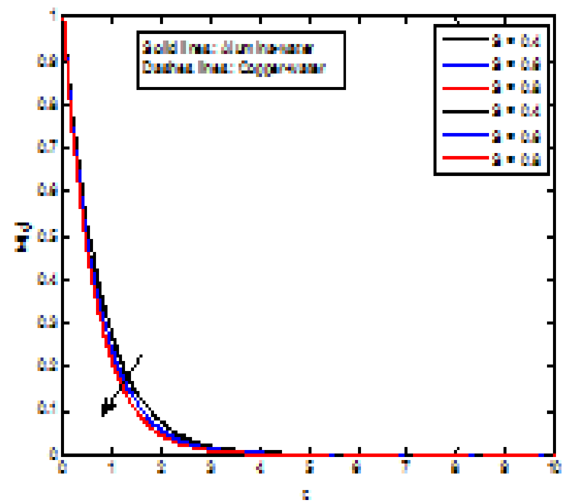

Figure 4: Variation of velocity profiles with S

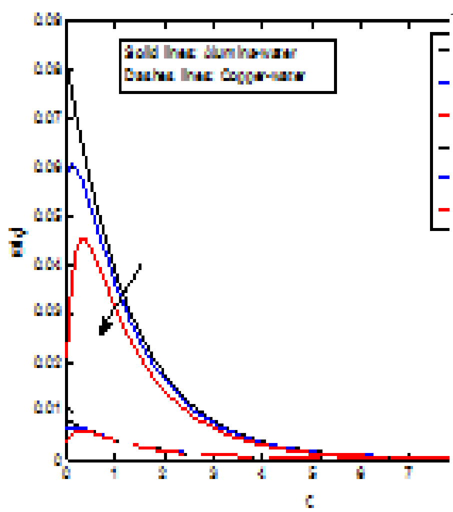

Figure 3: Variation of temperature profiles with k_1

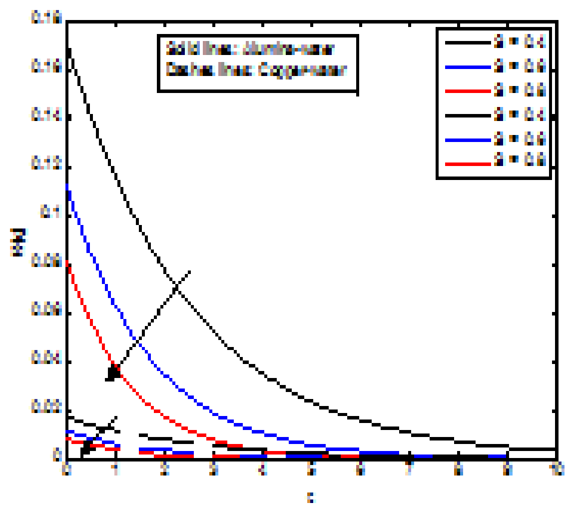

Figure 5:Variation of temperature

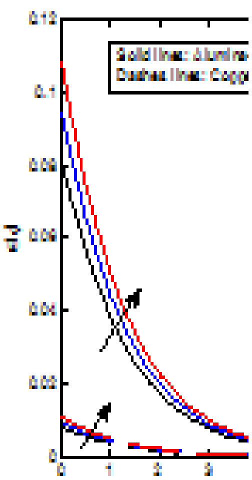

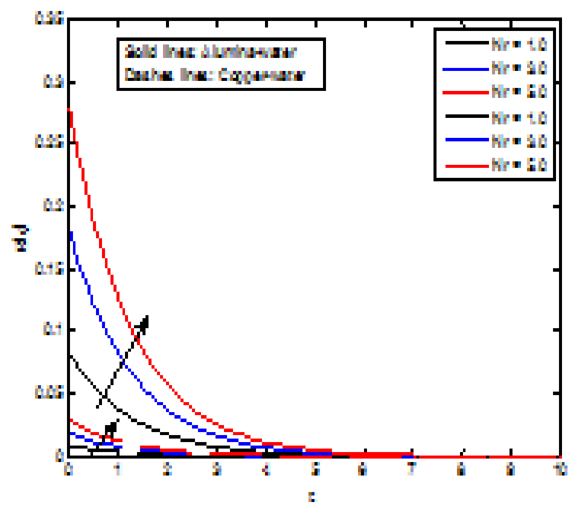

profiles with S

Figure 6: Variation of temperature profiles with Bn

Figure 8: Variation of Temperature profiles with Nr

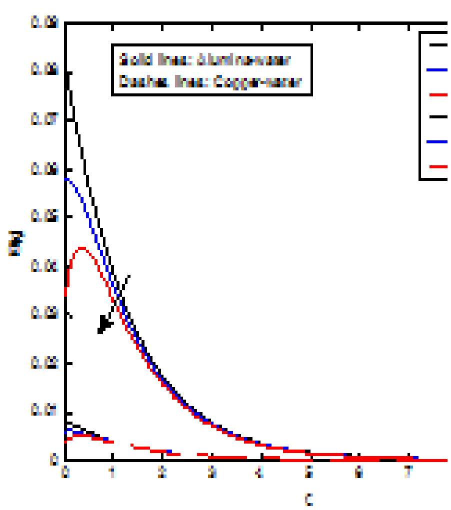

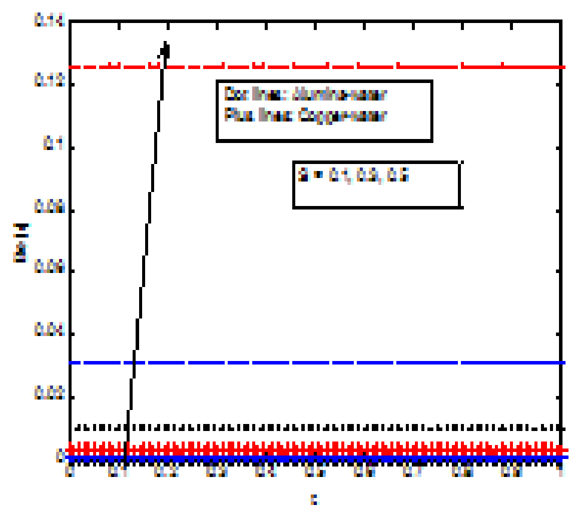

Figure 7: Variation of Temperature profiles with Ec
$Cu - water$ nanofluids.

Figure 9: The Bejan number with S

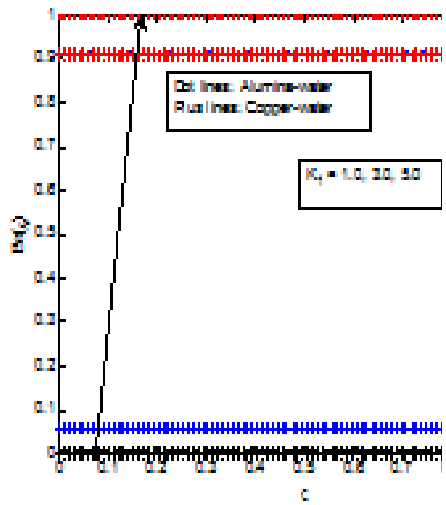

Figure 10: The Bejan number with k_1

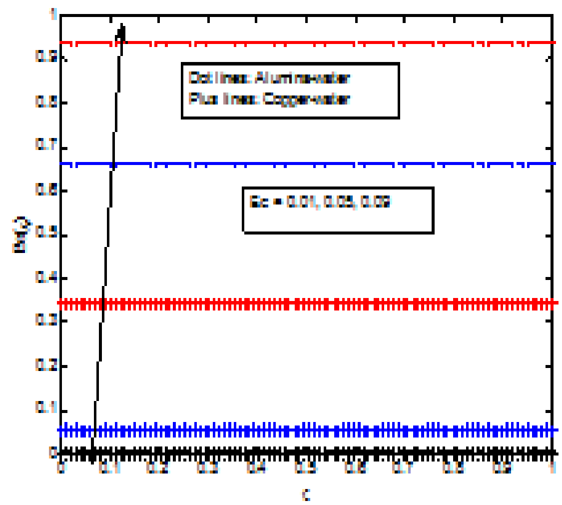

Figure 12: The Bejan number with Ec

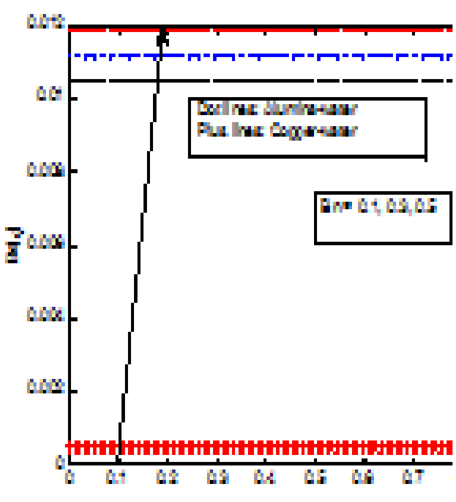

Figure 11: The Bejan number with Bn

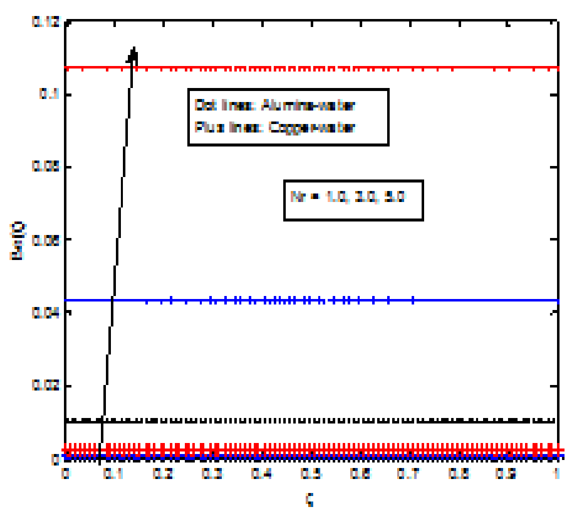

Figure 13: The Bejan number with Nr

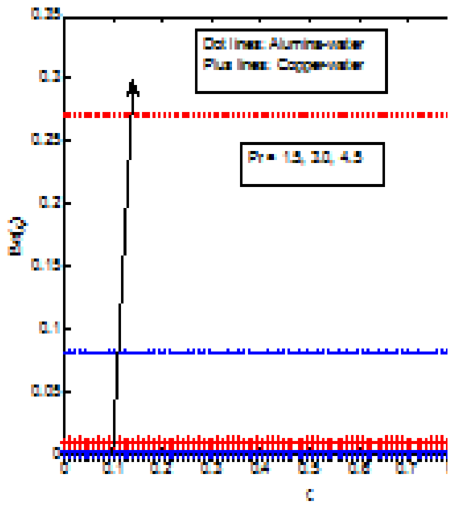

Figure 14: The Bejan number with Pr

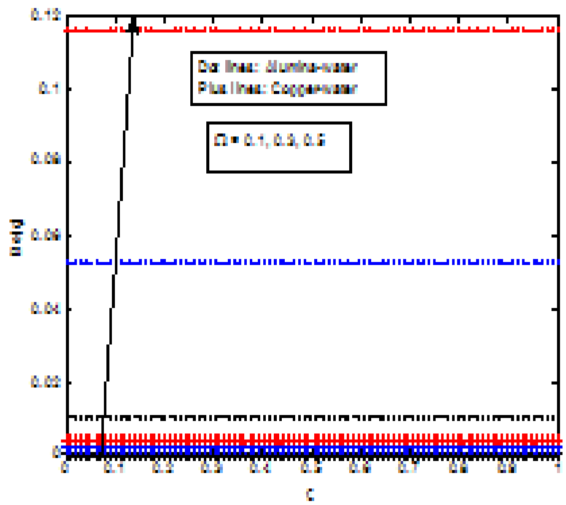

Figure 16: The Bejan number with Ω

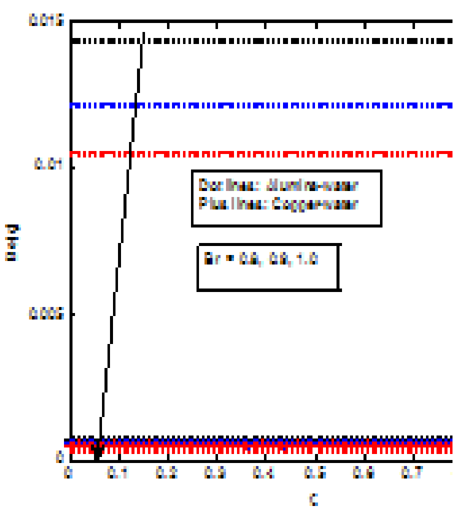

Figure 15:The Bejan number with Br

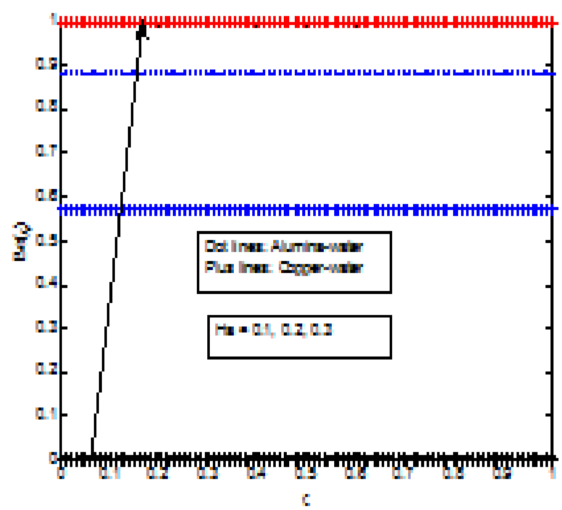

Figure 17: The Bejan number with Ha

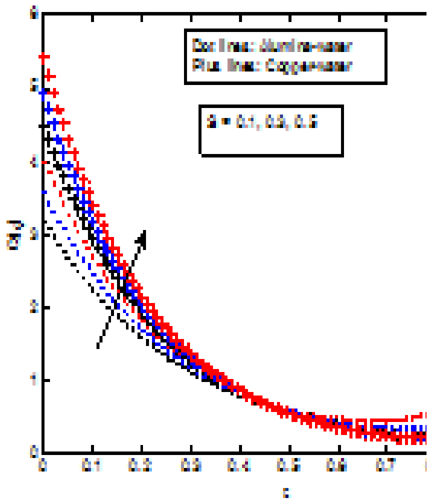

Figure 18: The Entropy number Vs ς for S

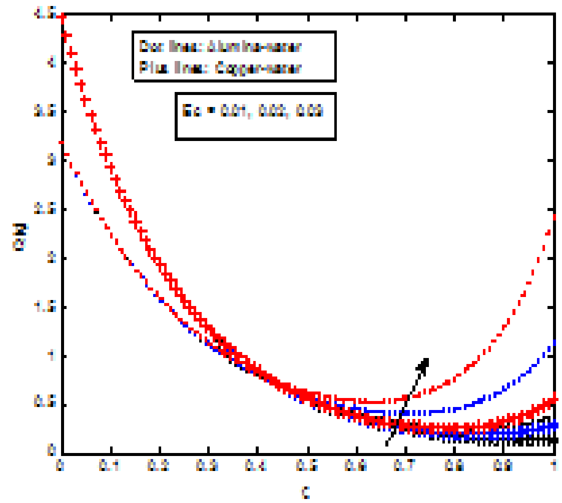

Figure 20: The Entropy number Vs ς for Ec

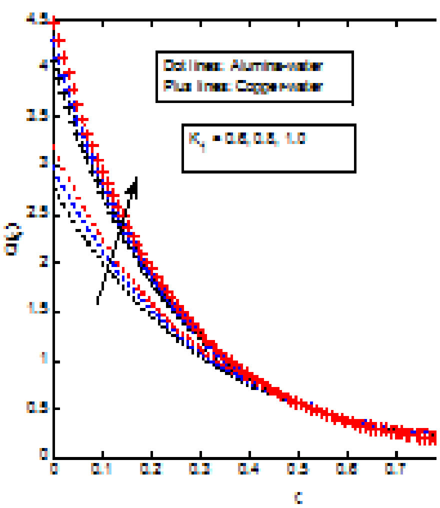

Figure 19: The Entropy number Vs ς for k_1

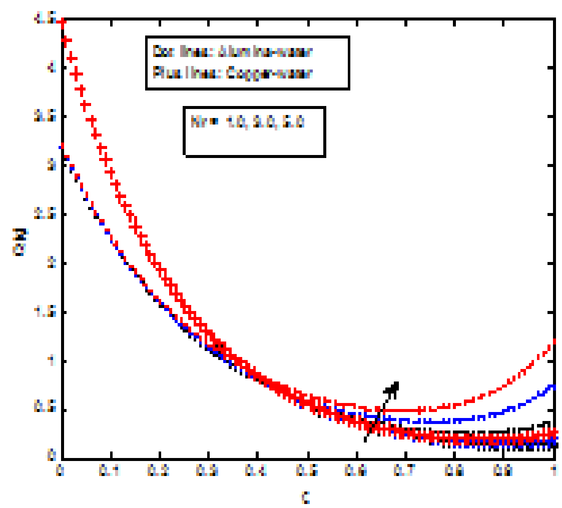

Figure 21: The Entropy number Vs ς for Nr

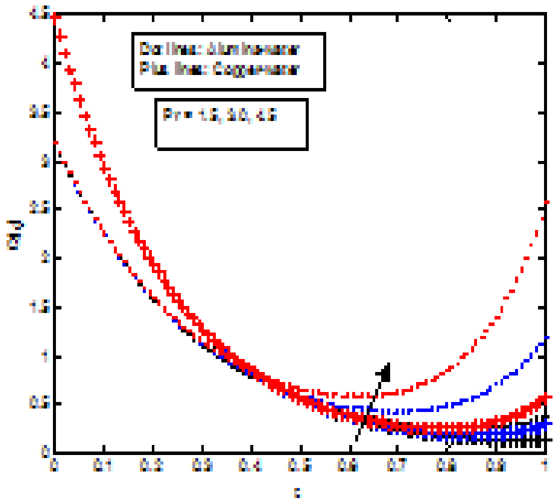

Figure 22: The Entropy number Vs ς for Pr

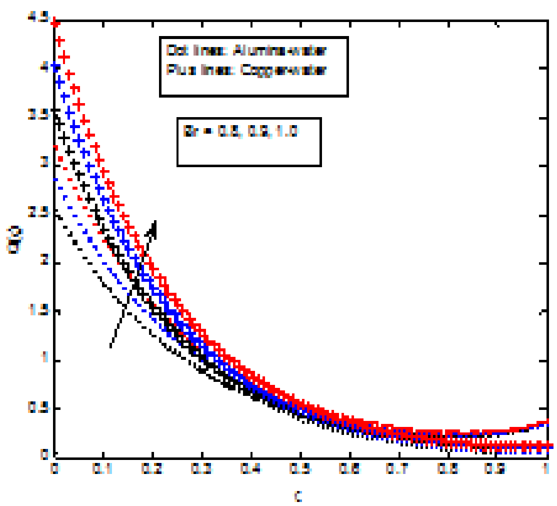

Figure 23:The Entropy number Vs ς for Br

Table 4: Variation of flow conditions and fluid properties on Bejan and entropy generation rate.

S	k_1	Bn	Ec	Nr	Pr	Br	Ω	Ha	Re	Al_2O_3water		Cu-water	
										Be Q		Be Q	
0.1										0.5647	0.5647	0.0568	0.0568
0.3										0.1782	0.1782	0.0174	0.0174
0.5										0.0981	0.0981	0.0981	0.0091
	0.1									0.5647	0.5719	0.0568	0.0572
	0.3									0.5066	0.5685	0.0542	0.0571
	0.5									0.4062	0.5647	0.05041	0.0568
		0.1								0.5647	0.5647	0.0568	0.05668
		0.3								0.6720	0.6720	0.0676	0.0676
		0.5								0.7793	0.7793	0.783	0.0783
			0.01							0.5647	0.5647	0.0568	0.0568
			0.05							0.4635	0.5141	0.0482	0.0547
			0.09							0.3623	0.5141	0.0396	0.0525
				1.0						0.5647	0.5647	0.0568	0.0568
				3.0						1.2202	1.2202	0.1238	0.1238
				5.0						1.8756	1.8756	0.1908	0.1908
					1.5					0.5647	0.5647	0.0568	0.0568
					3.0					1.0961	1.0961	0.1129	0.1129
					4.5					1.5940	1.5940	0.1682	0.1682
						0.8				0.5647	0.5647	0.0568	0.0568
						0.9				0.5647	0.5647	0.0568	0.0568
						1.0				0.5647	0.5647	0.0568	0.0568
							0.1			0.5647	0.5647	0.0568	0.0568
							0.3			0.5647	0.5647	0.0568	0.0568
							0.5			0.5647	0.5647	0.0568	0.0568
								0.1		0.5647	0.5852	0.0568	0.0587
								0.3		0.5101	0.5772	0.0521	0.0580
								0.5		0.4172	0.5647	0.0444	0.0568
									0.02	0.5647	0.5647	0.0568	0.0568
									0.06	0.5647	0.5647	0.0568	0.0568
									0.10	0.5647	0.5647	0.0568	0.0568

7. CONCLUDING REMARKS

This study presents an analytical solutions for the problem of impact of entropy generation on hydromagnetic nanofluid flow dispersed over a radiative vertical porous plate with Newtonian heating. The main findings are summarized as follows:
-Entropy generation are enhanced by Eckert number, radiation parameter, permeability parameter, suction , prandtl number and Brinkman number for both copper and alumina water.
-Entropy generation decreases by temperature parameter.
-Bejan number decrease as Brinkman increase for both copper and alumina water.
-Bejan number increases as Eckert number, radiation parameter, permeability parameter, suction, prandtl number and Brinkman number for both copper and alumina water.

ACKNOWLEDGEMENTS

The authors would like to thank the anonymous referees whose comments improved the original version of this manuscript.

NOMENCLATURE

p.10 p.80 a_1, a_2, a_3 Constants

Be Bejan number

Bn Biot number

Br Brinkman

Cp Specific heat at constant pressure

Ec Eckert number

Ha Hartman number

h_f Convective heat transfer coefficient

K Permeability of the medium

k^* Absorption coefficient

k_{1nf} Thermal conductivity of the nanofluid

k_f Thermal conductivity of the fluid

k_s Thermal conductivity of the solid

k_1 Porosity parameter

L Characteristics length

M Dimensionless velocity

Nn Nusselt number

Nr Radiation parameter

Pr Prandtl number

P_1 Heat transfer due to irreversibility

P_2 Entropy generation by the friction

Q Dimensionless entropy generation rate

q_w Heat flux

q_r Radiative flux

Re Reynolds number

S Suction/injection

S_{gen} The rate of generation of entropy

S_0 Entropy generation rate due to characteristic length

S_f Skin friction

T_0 Reference temperature

T_1 Temperature

T_f Fluid temperature

T_∞ Ambient temperature

u_i Velocity along x axis

u_0 Reference velocity

u_w Velocity along the wall

v Velocity along y axis

Greek

α_{1nf} Thermal diffusivity of nanofluid

β_0 Coefficient of volumetric expansion

σ_{1nf} Electrical conductivity of the nanofluid

σ_f Electrical conductivity of the fluid

σ_s Electrical conductivity of the solid

ρ_{1nf} Density of the nanofluid

ρ_f Density of fluid

ρ_s Density of the solid

μ_{1nf} Dynamic viscosity of the nanofluid

ξ Volume fraction

ν_{1nf} Kinematic viscosity of the nanofluid

τ_w Shear stress at the wall

$\Gamma_{1........8}$ Constant

Ω Dimensionless temperature parameter

Θ Dimensionless temperature

φ Irreversibility ratio

REFERENCES

[1] O. Ajala, P. Adegbite, S. F. Abimbade and A. M. Obalalu, *Thermal radiation and convective heating on hydromagnetic boundary layer flow of nanofluid past a permeable stretching surface*, International Journal of Applied Mathematics and Statistical Sciences, 8(2):43-58, (2019).

(1) M. Akbarzadeh, S. Rashidi, M. Bovand and R. Ellahi, *A sensitivity analysis on thermal and pumping power for the flow of nanofluid inside a wavy channel*, Journal of Molecular Liquid, 220:1-13, (2016).

(2) S. Alboud and S. Saouli, *Entry analysis for viscoelastic magnetohydrodynamic flow over a stretching suface*, International Journal of Non-Linear Mechanics, 45:482-489, (2010).

(3) H. Alfven, *Existence of electromagnetic-hydrodynamic waves*, National Publication Group, 150(3805):405-406, (1942).

(4) S. T. Aminossa dating and B. Ghasemi, *Natural convection cooling of a localised heat source at the bottom of a nanofluid - filled enclosure*, European Journal of Mechanics B fluid, 28:630-640, (2009).

(5) A. Bejan, *Entropy Generation Through Heat and Fluid Flow.* Wiley, New York, (1982).

(6) A. Bejan, Entropy Generation Minimization: *The Method of Thermodynamic Optimization of Finite-Size Systems and Finite-Time Processes*, CRC Press, Boca Raton, (1995).

(7) A. Bejan, Entropy generation minimazation: *The method of thermodynamic optimization of finite -size system and finite-time process*, CRS press, (1996).

(8) K. C. Brinkman, *The viscosity of concentrated suspensions and solutions*, Journal of chemical physics, 20: 571-581, (1952).

(9) J. Buongiorno, *Convective Transport in Nanofluids*, ASME, Journal of Heat Transfer, 128:240-250, (2006).

(10) S. U. S. Choi, *Enhancing thermal conductivity of fluids with nanoparticles*, Proceedings of the ASME International Mechanical Engineering Congress and Exposition, San Francisco, California, USA, 66:99-105, (1995).

(11) P. Datta, P. S. Mahapatra, K. Ghosh, N. K. Manna and S. Sen, *Heat transfer and entropy generation in a porous square enclosure in presence of an adiabatic block*, Transport in Porous Media, 111(2):305-329, (2016).

(12) H. Eshetu, and B. Shankar, *Heat and mass transfer in the boundary layer of unsteady viscous nanofluid along a vertical stretching sheet*, Journal of Computer Engineering, 1-17, (2014).

(13) A. I. Fagbade, B. O. Falodun, and A. J. Omowaye, *MHD natural convection flow of viscoelastic fluid over an accelerating permeable surface with thermal radiation and heat source or sink*: spectral homotopy analysis approach, Ain Shams Engineering Journal, 9(4):1029-1041, (2016).

(14) P. Keblinski, S. R. Phillpot, S. U. S. Choi, and J. A. Eastman, *Mechanism of Heat Flow in Suspensions of Nano-Sized Particles (Nanofluids)*, International Journal of Heat and Mass Transfer, (42): 855-863, (2002).

(15) W. A. Khan, and P. Pop, *Boundary Layer Flow of a Nanofluid past a Stretching Sheet*, International Journal of Heat and Mass Transfer, 53:2477-2483, (2010).
(16) L. B. Kish and D. K. Ferry, *Information entropy and thermal entropy*: apples and oranges, arXiv preprint arXiv:1706.01459, (2017).
(17) J. H. Merkin, *Natural-convection boundary-layer fow on a vertical surface with Newtonian heating*, International Journal of Heat and Fluid Flow, 15(5):392-398, (1994).
(18) A. Hussanan, I. Khan, and S. Shafe, *An exact analysis of heat and mass transfer past a vertical plate with Newtonian heating*, Journal of Applied Mathematics, 1-09 (2013).
(19) A. Hussanan, M. Z. Salleh, R. M. Tahar, and I. Khan, *Unsteady boundary layer flow and heat transfer of a Casson fluid past an oscillating vertical plate with Newtonian heating*, PloS one 9(10), e108763, (2014).
(20) D. Vieru, C. Fetecau, and N. Nigar, *Magnetohydrodynamic natural convection fow with Newtonian heating and mass difusion over an infnite plate that applies shear stress to a viscous fuid*, Zeitschriffor Natur for schung A69(12):714-724, (2014).
(21) Monaledi and Makinde, *Inherent irreversibility in cu-water nanofluid couette flow with variable viscosity and nonlinear radiative heat transfer*, International Journal of Fluid Mechanics Research, 46(6):525-543, (2019).
(22) G. P. Narayan, J. H. Lienhard and S. M. Zubair, *Entropy generation minimization of combined heat and mass transfer devices.* International Journal of Thermal. Science, 49(10):2057-2066 (2010).
(23) G. J. Oluwakuade, A. J. Omowaye and O. K. Koriko, *On the analysis of Navier slip and Newtonian heating on steady magnetohydrodynamics reacting convective fluid flow over a vertical plate*, International Journal of Engineering Applied Sciences and Technology, 4(5):93-99, (2019).
(24) A. J. Omowaye, *On Steady Free Convective Hydro Magnetic Flow of a Reactive Viscous Fluid in a bounded domain*, Pacific Journal of Science and Technology, 12(1):180-187, (2011).
(25) A. J. Omowaye, *Existence of solution for unsteady free convective reacting viscous flows on porous plate in presence of magnetic field*, Daffodil International University Journal of Science and Technology, 11(1):55-58, (2016).
(26) H. F. Oztop, and E. Abu-Nada, *Numerical study of convection in partially heated rectangular enclosures filled with nanofluids*, International Journal of Heat and fluid flow, 29(5):1326-1336, (2008).
(27) M. Ramzan, *Influence of Newtonian Heating on Three Dimensional MHD Flow of Couple Stress Nanofluid with Viscous Dissipation and Joule Heating*, PLoS ONE 10(4):e0124699, (2015).
(28) A. Sahoo, and R. Nandkeolyar, *Entropy generation and dissipative heat transfer analysis of mixed convective hydromagnetic flow of a Casson nanofuid with thermal radiation and Hall current*, Scientific Reports 11:3926-3957, (2021).
(29) M. Sheikholeslami, D. D. Ganji, M. Y. Javed and R. Ellahi, *Effect of thermal radiation on magnetohydrodynamics nanofluid flow and heat transfer by means of two phase model*, Journal of Magnetic and Magnetism Material, 374:36-43, (2015).
(30) L. C. Woods, *Thermodynamics of Fluid Systems*, Oxford, UK: Oxford University Press, (1975).
(31) N. A. Zainal, R. Nazal, K. Naganthran and I. Pop, *MHD flow and heat transfer of hybrid nanofluid over a permeable moving surface in the presence*

of thermal radiation, International Journal of Numerical Methods for Heat and Fluid Flow, 1-22, (2020).

DEPARTMENT OF MATHEMATICAL SCIENCES, FEDERAL UNIVERSITY OF TECHNOLOGY, AKURE, NIGERIA
E-mail address: ajomowaye@futa.edu.ng
DEPARTMENT OF MATHEMATICAL SCIENCES, FEDERAL UNIVERSITY OF TECHNOLOGY, AKURE, NIGERIA
E-mail address: okkoriko@futa.edu.ng